Spontaneous breaking and re-making of the RS-Au-SR staple in self-assembled ethylthiolate/Au(111) interface

Gao, Jianzhi; Li, Fangsen; Zhu, Gangqiang; Yang, Zhibo; Lu, Hongbing; Lin, Haiping; Li, Qing; Li, Youyong; Pan, Minghu; Guo, Quanmin

DOI:
10.1021/acs.jpcc.8b04157
10.1021/acs.jpcc.8b04157

Document Version
Peer reviewed version

Citation for published version (Harvard):
Gao, J, Li, F, Zhu, G, Yang, Z, Lu, H, Lin, H, Li, Q, Li, Y, Pan, M & Guo, Q 2018, 'Spontaneous breaking and re-making of the RS-Au-SR staple in self-assembled ethylthiolate/Au(111) interface', *Journal of Physical Chemistry C*, vol. 122, no. 34, pp. 19473−19480. https://doi.org/10.1021/acs.jpcc.8b04157, https://doi.org/10.1021/acs.jpcc.8b04157

Spontaneous Breaking and Re-making of the RS-Au-SR Staple in Self-assembled Ethylthiolate/Au(111) Interface

*Jianzhi Gao[1§], Fangsen Li[2§], Gangqiang Zhu[1], Zhibo Yang[1], Hongbing Lu[1], Haiping Lin,[*3] Qing Li,[3] Youyong Li,[3] Minghu Pan[*4] and Quanmin Guo[*5]*

[1] *School of Physics and Information Technology, Shaanxi Normal University, Xi'an 710119, China*

[2]*Suzhou Institute of Nano-Tech and Nano-Bionics, SEID, Suzhou Industrial Park, Suzhou, Jiangsu Province, 215123, China*

[3]*Institute of Functional Nano & Soft Materials, Jiangsu Key Laboratory for Carbon-Based Functional Materials & Devices, Soochow University, 199 Ren-Ai Road, Suzhou, Jiangsu Province, 215123, China*

[4]*School of Physics, Huazhong University of Science and Technology, Wuhan 430074, China.*

[5]*School of Physics and Astronomy, University of Birmingham, Birmingham B15 2TT, United Kingdom*

Abstract: *The stability of self-assembled RS-Au-SR (R = CH_2CH_3) /Au(111) interface at room temperature has been investigated using scanning tunneling microscopy (STM) in conjunction with density functional theory (DFT) and MD calculations. The RS-Au-SR staple, also known as Au-adatom-dithiolate (AAD), assembles into staple rows along the* $[11\bar{2}]$ *direction. STM imaging reveals that while the staple rows are able to maintain a static global structure, individual staples within the row are subject to constant breaking and remaking of the Au-SR bond. The C_2S-Au-SC_2/Au(111) interface is under dynamic equilibrium and it is far from rigid. DFT/MD calculations show that a transient RS-Au-Au-SR complex can be formed when a free Au atom is added to the RS-Au-SR staple. The relative high reactivity of the RS-Au-SR staple at room temperature could explain the reactivity of thiolate-protected Au nano-clusters such as their ability to participate ligand-exchange and intercluster reactions.*

[*] Correspondence and requests for materials relating to modelling should be addressed to Dr H-P Lin, email: hplin@suda.edu.cn. For information relating to experiment, Dr. M Pan, email: minghupan@hust.edu.cn and Dr Q Guo, email: Q.Guo@bham.ac.uk.

Introduction

Self-assembled monolayers (SAMs)[1-6] of alkanethiol molecules have been extensively studied during the last three decades as a model system for smart surface engineering and nanotechnology. A well-known application of such SAMs is the passivation and stabilization of gold nano-particles.[7,8] Early studies on Au(111) using surface-related techniques[9-22] suggested that –SR (R= -$(CH_2)_nCH_3$) is the basic unit attached directly to an unreconstructed Au(111) surface. This early understanding has been challenged by the discovery of Au-adatom-dithiolate (RS-Au-SR) from both scanning tunneling microscopy (STM) imaging[23] on Au(111) and high-resolution x-ray diffraction[7] of thiol-coated Au nanoparticles. Recent investigations have greatly improved our understanding of the RS-Au system.[24-42] So far, imaging with the STM has clearly identified the existence the RS-Au-SR motif for monolayers of both the simple akylthiolates such as methylthiolate,[23,30,32] ethylthiolate,[26,30] propylthiolate[43] and phenylthiolate,[44] and the more complex thiolates such as 1,3,5-tris(4-mercaptophenyl) benzene[45] on Au(111). The involvement of the Au-adatom and the formation of the RS-Au-SR-like motif seem to depend on the structure of the gold crystal plane. For example, a recent investigation suggests that the bonding between mercaptobenzoic acid and the Au(110) surface does not involve Au-adatoms.[37] The structure of R in SR also affects the binding of SR to the gold substrate. [41]

Therefore, the stability of alkanethiol SAMs is an important issue to consider when they are used either to protect gold nanoparticles or as a passivation layer for a metal against corrosion. Previous studies have shown that when a gold single crystal with a thiolate monolayer is brought into contact with a diakyl disulfide solution, the surface thiolate can be substituted by molecules from the solution.[46] Such a ligand exchange reaction has also been observed to occur on the surface of gold nanoparticles.[47] A recent high-resolution STM study in conjunction with density functional theory (DFT) calculations has attempted to explain how one of the RS branches in RS-Au-SR can be replaced.[48] Here, we present the findings from our recent study of the CH_3CH_2S-Au-SCH_2CH_3 (C_2S-Au-SC_2) SAM on the Au(111) surface. We have observed, via direct imaging with the STM, the breaking and re-making of the S-Au bond. DFT calculations reveal that at RT there is a finite probability for one of the $–SC_2$ units to leave the C_2S-Au-SC_2 staple if there is a Au adatom in the vicinity. By incorporating an extra Au adatom into a C_2S-Au-SC_2 staple, a (C_2S-Au-Au-SC_2) complex can be formed. The complex can further decompose giving rise to two Au-adatom-monothiolate (C_2S-Au) species.[35] The spontaneous breaking and re-making of the S-Au bond mediated by the Au adatom at RT may play an important role in previously reported ligand exchange reactions[47] and inter-cluster interactions[8] involving thiol-

protected Au nanoparticles. Our finding further emphasizes the importance of the dispersive interaction among the alkane chains in stabilizing the SAM because the S-Au bond is vulnerable to thermally induced rupture at RT. The notion "thiolate" has been widely used in literature, [40] although a recent study has suggested that S is in the radical thiyl state. We have decided to follow the tradition in the literature and use the term thiolate for adsorbed –SR.

Methods

The experiments are conducted in an ultra-high vacuum (UHV) chamber with a base pressure of 5×10^{-10} mbar using an Omicron variable temperature STM (VT-STM). The gold sample is a (111)-oriented Au film deposited on a highly oriented pyrolitic graphite substrate. The C_2S-Au-SC_2 monolayer is prepared by exposing the clean gold sample to 1×10^{-5} mbar of ethanethiol vapor at RT in vacuum. Initially, a full coverage of ethylthiolate with a coverage of 1/3 monolayer (ML) is prepared on the Au(111) substrate. Subsequent thermal annealing under UHV leads to gradual reduction of the surface coverage via thermal desorption and the change of surface structure from (3 × 4) to various striped phases.[26]

The DFT calculations were performed with the Vienna *ab initio* Simulation Package

(VASP).[49,50] The electron-ion interactions were described using the projected augmented wave (PAW) method.[51] The exchange-correlation energy was calculated with the general gradient approximation (GGA) functionals of Perdew-Burke-Ernzerhof (PBE).[52] An energy cutoff of 400 eV was selected for the plane-wave expansion. The dispersion corrections of the molecules and Au surface interactions were included by the van der Waals density functional (vdw-DF) proposed by Dion.[53-55] The Au surfaces were modeled with periodic slabs consisting of five atomic layers. A vacuum of 15 Å was adopted to avoid the periodic image interactions normal to the surface. A Monkhorst-Pack grid of 2 × 4 × 1 was employed to sample the surface Brilloun zone. In all cases, the top three layers of atoms were allowed to relax in three dimensions. The first principles STM simulations were conducted with the Tersoff-Hamann method and the bSKAN code.[56,57] The molecular dynamics (MD) simulations were performed at 300 K with *NVT* ensemble. The simulation time was 1000 fs with a time step of 1 fs.

Results and discussion

Both the full coverage (3 × 4) phase and various low coverage striped phases C_2S-Au-SC_2 on Au(111) have been reported and discussed in detail in a previous publication. [26] Here we focus on one of the striped phases, (6√3 × √3)-R30°, which consists of

rows of C_2S-Au-SC_2 aligned in the $[11\bar{2}]$ direction. In the orthogonal $[1\,\bar{1}0]$ direction, the period of the rows is 9*a* where *a* is the nearest neighbor distance of surface Au atoms. Figure 1a and b shows STM images from such a striped phase at RT, with a corresponding ball model shown in Fig. 1c. The $(6\sqrt{3} \times \sqrt{3})$-R30° phase has a coverage of 0.23 ML and is achieved by thermally desorbing 0.1 ML of adsorbate from the dense 3 × 4 phase which has a coverage of 1/3 ML.[26] This is done by heating the sample to 378 K. As can be seen in Fig. 1c that the C_2S-Au-SC_2 rows appear in pairs. The distance between two paired-rows along the $[1\,\bar{1}0]$ direction is 3.5*a* while the distance between two neighboring pairs is 9*a*. Each C_2S-Au-SC_2 is characterized by two protrusions in the STM image, arising from the two ethyl branches. The two protrusions from each C_2S-Au-SC_2 are separated by a typical distance of 0.65 nm. As shown in Fig. 1c, because of the pairing of C_2S-Au-SC_2, the two ethyl branches on the opposite sides of the Au adatom are in symmetry nonequivalent positions and hence they appear with different heights.[26] Each C_2S-Au-SC_2 in Fig. 1a and b has an α branch and a β branch. The pairing of C_2S-Au-SC_2 follows a head-to-head scheme where the β branch from one C_2S-Au-SC_2 sits next to the β branch of another C_2S-Au-SC_2 (Fig. 1c). These two β branches are separated by a rather short distance of ~ 0.3 nm.[26] The distance between the α and β branch of the same C_2S-Au-SC_2 unit is ~0.65 nm.[26] The presence of the C_2S-Au-SC_2 units on

the Au(111) surface is consistent with the staple motif used to describe the gold-thiolate interface for thiol passivated Au nanoparticles.[7, 38]

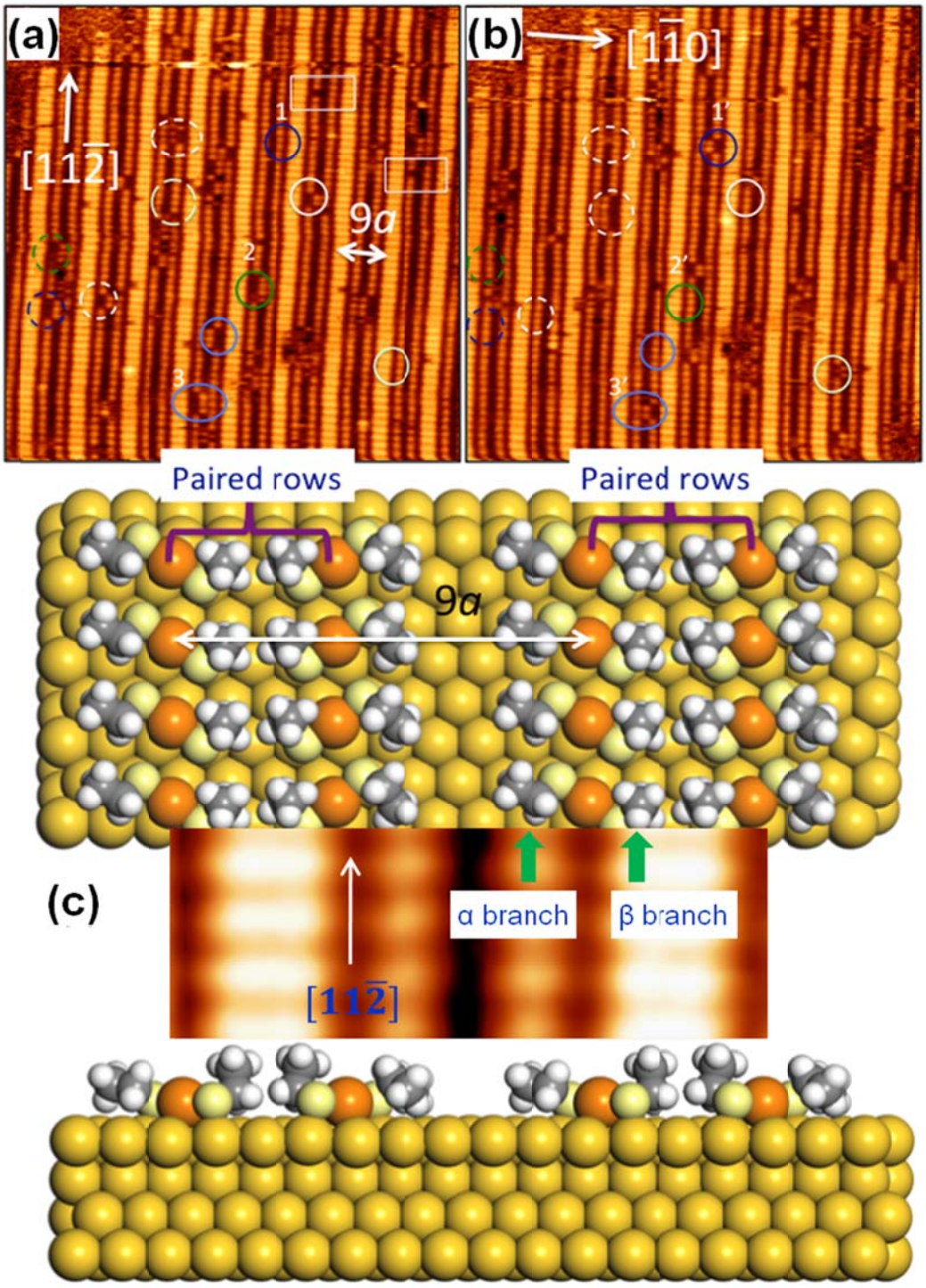

Figure 1. (a) STM image, 25 nm × 25 nm, from a (6√3 × √3)-R30° striped phase of C_2S-Au-SC_2 obtained at RT with 2.0 V bias voltage and 0.3 nA tunnel current. The stripes have a period of *9a* in the $[1\,\bar{1}0]$ direction. Each C_2S-Au-SC_2 shows two spots

in STM corresponding to the two C_2S branches. (b) STM image, 25 nm × 25 nm, taken from the same area as that of (a) three minutes later. Circles highlight locations where clear changes are observed between the two images. (c) Structural model verified by DFT of the $(6\sqrt{3} \times \sqrt{3})$-R30^o striped phase. Both the planar and the cross sectional views are given. Orange spheres are Au adatoms; light yellow spheres are S atoms; grey spheres are C atoms and white spheres are hydrogen atoms. A section of the STM image taken from (a) is overlaid onto (c) so that a direct comparison between the protrusions in STM images and the locations of ethyl chains can be made. For each C_2S-Au-SC_2, there are two nonequivalent R branches: the α branch and the β branch with the β branch appearing taller in the images.

The two STM images in Fig. 1 are collected from the same area of the sample at RT, with image in Fig. 1b acquired three minutes' later than that in Fig. 1a. Direct comparison between the images shows that there is a stable global structure defined by the C_2S-Au-SC_2 rows giving an impression that the $(6\sqrt{3} \times \sqrt{3})$-R30^o does not change with time. However, a closer inspection reveals that local changes within each row take place constantly. Circles and ovals added to the images highlight a number of locations where changes have been observed. For clarity, we have not labeled all locations in the figure where changes are observed. The change is identified as a characteristic lateral translation of the α branch. For example, by comparing the area inside the blue circle *1* in Fig. 1a and that inside the blue circle *1'* in Fig. 1b, we notice that two dots corresponding to two α branches have shifted sideways to the left by ~0.25 nm during the interval of acquiring the two images. This sideway shift gives an impression that the staple has been stretched from its initial length of 0.65 nm to

0.9 nm. Inside the green circle *2* in Fig. 1a, three α branches are seen to be in the "stretched" position. When Fig. 1b is collected, the same α branches are observed to have returned to their usual, non-stretched, positions. Inside the blue oval *3* in Fig. 1a there are again three stretched α branches with the same displacement to the right. In Fig. 1b, it can be seen that these three stretched α branches have returned to their normal positions. During the same time interval, two α branches from the neighboring row on the right hand side have displaced to the left.

As we continuously image the same area, we find this "stretching" and "restoring" process occurring at random locations along the C_2S-Au-SC_2 row. In fact, the process is frequent enough such that we can capture a single "stretching" or "restoring" step in real time. As will be discussed later, the "stretching" and "restoring" are two steps of one reversible process involving the lateral displacement of the α branch. There is no real physical stretching of the molecular bond. In Fig. 2a, as the tip scans from the bottom of the image upwards, an α branch is observed to suddenly shift from its initial position, pointed by a white arrow, to a new "stretched" position pointed by a blue arrow. The same branch is thus seen by the STM at two different locations before and after the displacement. The displacement occurs after the STM tip has scanned through ~1/3 of the branch with 2/3 of the branch seen at the new location. Similarly

in Fig. 2b, an α branch is captured to move from the "stretched' position back to the normal position. The sudden appearance of straight lines, such as those seen in Fig. 2 a and b, in STM images is frequently associated with tip-induced movement. It is not always possible to distinguish thermal effect from tip-induced effect when molecules/atoms have gone through a displacement. However, the stretching and restoring phenomenon shown in Figs. 1 and 2 is mainly thermally excited. This is because we observe a large number of movements in between two frames, but only a small fraction of those movements are in conjunction with the appearance of straight lines, i.e., most of the changes take place when the STM is far away from the location of the event.

We performed STM simulation searching for the final state of C_2S-Au-SC_2 after it has been "stretched", by considering the incorporation of a Au adatom into the staple. The simulation is performed on an unreconstructed Au(111) because the herringbone reconstruction is lifted in the presence of ethylthiolates. The simulation begins with a single Au adatom sitting in the vicinity of a C_2S-Au-SC_2 staple. The final structure and simulated STM image are shown in Fig. 2(c) and (d), respectively. The calculated image shows the bright protrusions for the paired β branch rows, consistent with the STM images. In Fig. 2(c), one of the C_2S-Au-SC_2 staples has changed into C_2S-Au-

Au-SC_2 after capturing the Au adatom. The distance between the two C_2S branches in C_2S-Au-Au-SC_2 is longer than that within the C_2S-Au-SC_2 staple. The four snap shots in Figure 3 show how an isolated Au adatom becomes incorporated into a C_2S-Au-SC_2 staple.[58]

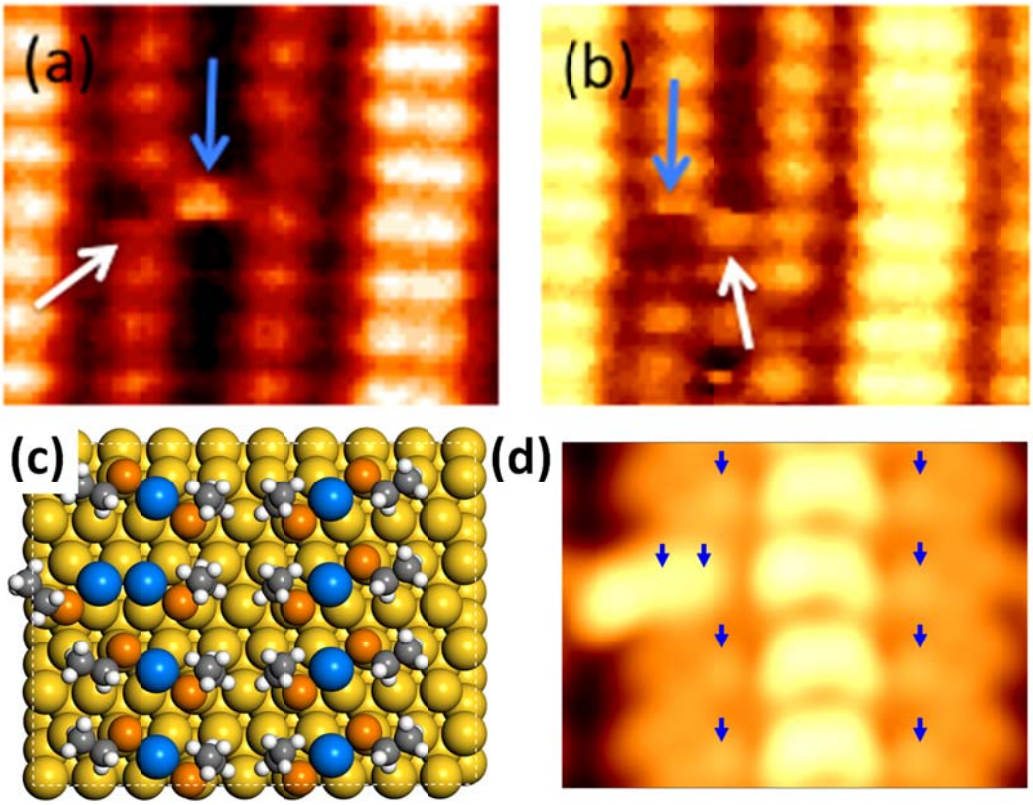

Figure 2. STM images demonstrating the real time capturing of the moving α branch. (a) A branch located in its normal position, pointed by a white arrow, translates sideways to a new location, pointed by a blue arrow. Bias: 2.0 V; tunnel current: 0.3 nA. (b) The reverse process where an α branch moves from the stretched position back to the normal position. The structure (c) and the simulated STM image (d) of the final state of the "stretched" process, mediated through incorporating a Au adatom into a staple. The simulated STM image corresponds to the same experimental condition of 2.0 V and 0.3 nA. The Au adatoms are illustrated as blue balls in (c) and pointed by blue arrows in (d).

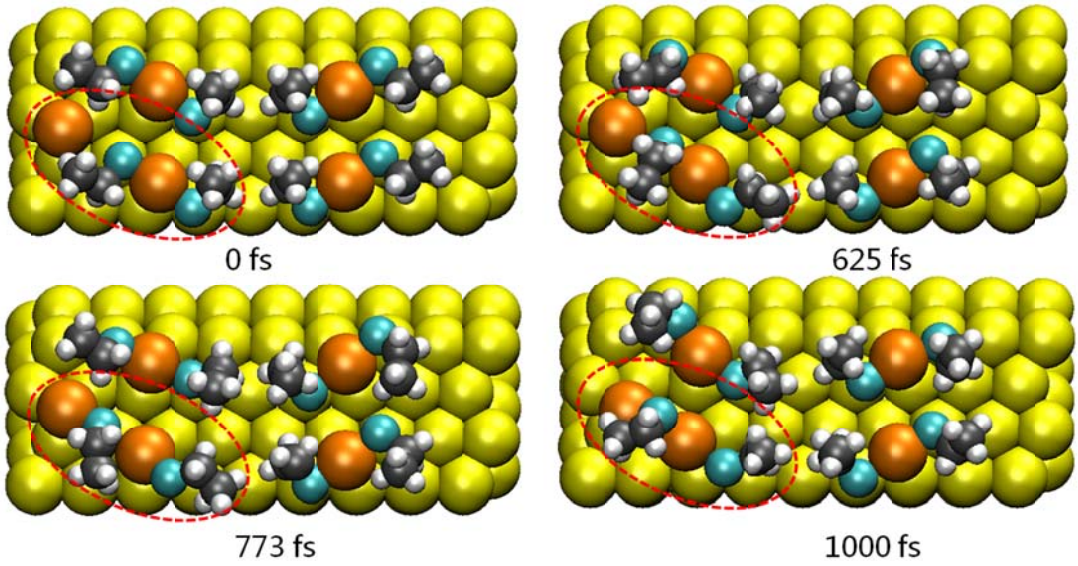

Figure 3. Four panels of snapshots at the simulation time of 0 fs, 625 fs, 773 fs, and 1000 fs, respectively. The dynamic S-Au bond formation and dissociation is highlighted with red ovals. A movie of the simulation can be found in the Supplementary Information.

The simulation shows that the displacement of the α branch observed with the STM can be explained by considering the transformation from C_2S-Au-SC_2 to C_2S-Au-Au-SC_2 via the following scheme.

$$C_2S\text{-Au-}SC_2 + Au = C_2S\text{-Au-Au-}SC_2 \qquad (1)$$

We now discuss and compare with other possible physical processes that may lead to the "stretching" and "restoring" of the C_2S-Au-SC_2 staple. In principle, a simple conformational change of the C_2 chain can introduce an extra distance between the two methyl groups within one staple. However, the change of distance observed here is too large for conformational variations. Moreover, conformational changes are observed only under very low bias voltage.[59] The relatively large displacement

exhibited by the α branch can only be explained by a true physical translation of this branch. There is the possibility that the C_2S-Au-SC_2 staple breaks apart according to the following scheme.

$$C_2S\text{-Au-}SC_2 = C_2S\text{-Au} + \text{-}SC_2 \qquad (2)$$

As can be seen in Fig. 1c, there is a narrow channel with exposed Au atoms in between adjacent pairs of staple rows. Following bond breaking, -SC_2 can move sideways to form a bond with the exposed Au atoms. In a study of hybridization of phenylthiolate and methylthiolate on Au(111), Maksymovych *et al* calculated the energy barrier for breaking the S-Au bond. They found an energy barrier of ~16.6 kcal/mole for breaking the S-Au bond of CH_3S-Au-SCH_3 and 15.9 kcal /mole in the case of PhS-Au-SPh, suggesting that at RT breaking the S-Au bond is a possible reaction.[48] It is very difficult to distinguish the above two schemes based on the STM images. However, there is a significant difference between the above two schemes. According to scheme (1), the positions of the two -SC_2 branches in C_2S-Au-Au-SC_2 are strictly correlated. In contrast, -SC_2, after breaking away from C_2S-Au-SC_2 according to scheme (2), has plenty of freedom to move. From Fig. 1 (c), we can see a narrow channel, about three Au atoms wide, of exposed Au atoms in between the thiolate rows. Within this channel, there are more than one adsorption sites that can accommodate the breakaway -SC_2. Thus, we expect more than one possible distance

between this -SC_2 and the residue of the broken staple -$AuSC_2$. STM images, Fig. 4 (a) and (b) for example, show that the displaced α branch has only one fixed location relative to the initial staple. Thus, scheme (1) is a more realistic option than (2). C_2S-Au-Au-SC_2 can be formed by either inserting a Au atom into C_2S-Au-SC_2, or by joining two Au-SC_2 together. Figure 4 (c) shows an interesting phenomenon suggesting the formation of C_2S-Au-Au-SC_2 rows. In this figure, the 0.65 nm distance covered by the red arrow in between the blue lines is the typical distance between the α and the β branch of a C_2S-Au-SC_2 staple. The 0.9 nm distance covered by the purple arrow in between the green lines is the longer distance between the displaced α branch and the β branch it was associated with before the displacement. This distance corresponds to the distance between the two methyl groups in C_2S-Au-Au-SC_2. In Fig. 4(c), one can find two occasions where a C_2S-Au-SC_2 row sitting right next to a C_2S-Au-Au-SC_2 row. The image in Fig. 4(c) provides further evidence supporting scheme (1).

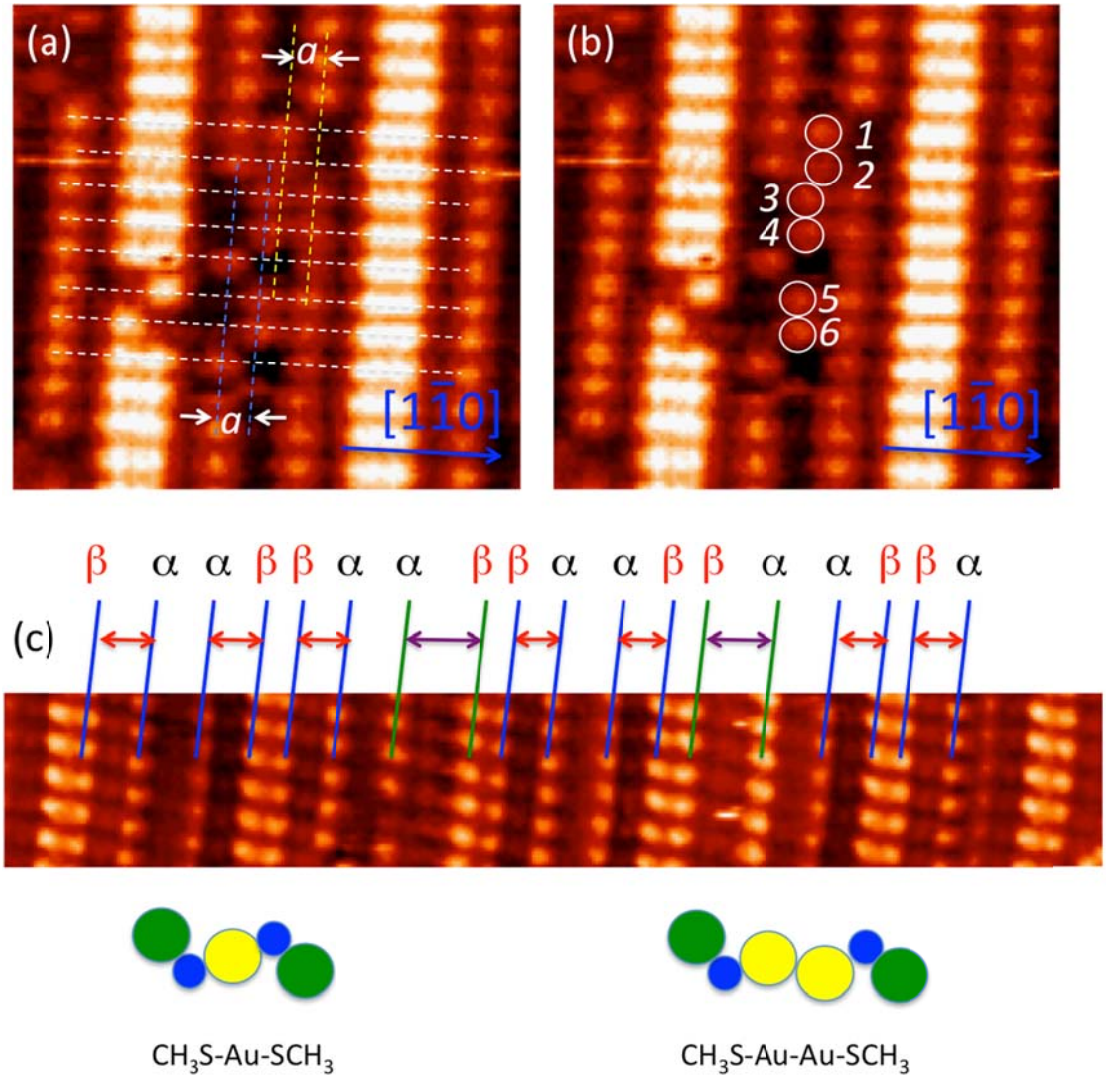

Figure 4. (a) The displaced α branch takes a rather specified location relative to the $(6\sqrt{3} \times \sqrt{3})$-R30° lattice. The displacement can be quantified by a translation along the $[1\,\bar{1}0]$direction by 1*a*, where *a* is the nearest neighbor distance for Au atoms. (b) 1 and 2 are two α branches displaced from the right to the left; 3, 4,5, and 6 are four α branches displaced from the left to the right. (c) Extended C_2S-Au-Au-SC_2 rows running parallel to C_2S-Au-Au-SC_2 rows. The image is slightly distorted because of uncorrected skew.

Both experiment and MD calculations provide the evidence that the C_2S-Au-SC_2 staple is under dynamic equilibrium at RT on Au(111). The staple can break and re-

shape. For the ($6\sqrt{3} \times \sqrt{3}$)-R30^{o} phase, there is a narrow channel of exposed Au atoms. The space provided by this channel can accommodate a displaced α branch from the left or the right, but not from both sides. Inspired by this vision, we studied the stability of the C_2S-Au-SC_2 staple in other phases. No displacement of either the α or the β branch can take place within the full coverage, (3 × 4) phase of C_2S-Au-SC_2, which has been demonstrated clearly in our previous work[26]. Figure 5 shows the STM images for typical ($5\sqrt{3} \times \sqrt{3}$)-R30° striped phase and full coverage (3 × 4) phase. The ($5\sqrt{3} \times \sqrt{3}$)-R30° striped phase is obtained by thermal annealing the sample with the (3 × 4) phase to 325 K. Neither the ($5\sqrt{3} \times \sqrt{3}$)-R30° nor the (3 × 4) phase shows any sign of displacement of the α or the β branch at RT. These results suggest, two factors have to be fulfilled for spontaneous S-Au bond breaking/remaking: 1. a channel of exposed Au atoms. 2. the channel must be wide enough to accommodate a displaced α branch. Otherwise, the C_2S-Au-SC_2/Au(111) interface is stable. It is also expected that for thiol molecules with a longer alkane chain, the stronger van der Waals interaction between the chains would give rise to a stronger restoring force and hence make the staple more stable. Alkanethiol SAMs with practical applications are those from molecules with eight CH_2 groups or more. In such cases, the van der Waals interaction among the alkane chains provides an important stabilizing factor for the SAM, while the relatively weak S-Au bond still allows effective ligand exchange.

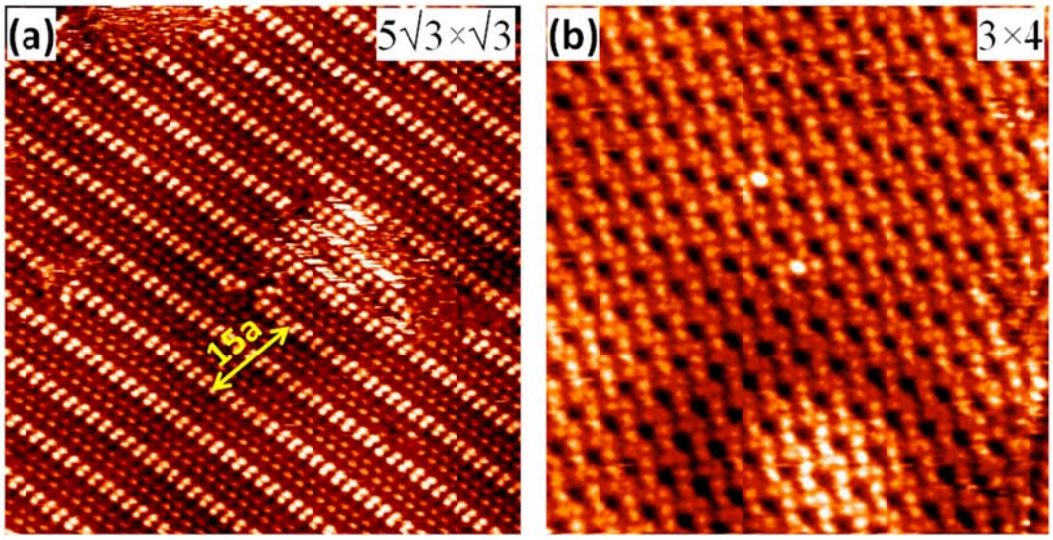

Figure 5. (a) STM image, 25 nm × 25 nm, obtained from a (5√3 × √3)-R30° striped phase of C_2S-Au-SC_2 at RT with 2.0 V sample bias and 0.3 nA tunnel current. The stripes have a period of *15a*. (b) STM image, 12 nm × 12 nm, taken from a (3 × 4) phase of full coverage C_2S-Au-SC_2. Both phases form at different coverages. STM images were obtained by using -0.6 V sample bias and 0.5 nA tunneling current.

Since the breaking and remaking of the S-Au bond involves Au atoms, a natural question to ask is where do these Au atoms come from? It has been known for sometime that on the close-packed surfaces of fcc metals, there is a low concentration of individual metal atoms. These atoms come from the step edges and can diffuse rather freely on the surface. It can be viewed as a simple vaporization and condensation process with the steps serving as a source of atoms. The concentration of these diffusing atoms depends on sample temperature. The rate of "vaporization" at step edges depends on step energy which itself is influenced by molecular adsorption. Under our experimental conditions, the step edges are expected to be decorated by thiolates. There is thus the possibility that Au atoms from step edges are extracted in

the form of Au-SR or RS-Au-SR.

One thing that we have not discussed yet is the defect-like feature observed along the paired bright β rows. As can be seen in Figs. 1 a and b, there are a very small number of missing β chains in each image. The defect is not permanently located at one position and seems to move. The defect gives an impression that a β chain is missing from the expected position. However, it is possible that nothing is really missing. What we observe may be due to a temporary breaking of a S-Au bond at the β chain. The consequence of such a bond break is to generate a free –SR which may resume its bonding with the Au adatom and restore the C_2S-Au-SC_2 staple. The rare occurrence of the β chain is also observed for the, denser, (5√3 ×√3)-R30° phase. In Fig. 4a, there are a few dim or missing β chains. We cannot exclude the possibility that the missing β chain is due to a methylthiolate impurity.

Conclusions

In summary, we have directly observed spontaneous S-Au bond breaking and bond remaking at RT within a self-assembled monolayer of C_2S-Au-SC_2. We have found that free-diffusing Au adatoms can be efficiently inserted into the C_2S-Au-SC_2 staple by forming a transient C_2S-Au-Au-SC_2 complex. Thermally induced reaction in which C_2S-Au-SC_2 breaks apart into C_2S-Au and SC_2 is also possible. We have identified

that the structure of the SAM has a strong influence on the stability of the SAM. Steric hindrance within a denser layer retards the bond breaking process. Although the staple motif has been widely accepted as the building block for alkanethiol self-assembled monolayers on the surface of Au(111) as well as on the surface of gold nano-particles, the initial assembly process leading to the formation of the staple layer still requires further clarification. Future work will help to understand how the concentrations of -SR, Au-SR, RS-Au-SR, and Au adatoms change with temperature. The roles of –SR and Au-SR in particular, require further investigation.

ASSOCIATED CONTENT

Supporting Information

Supplementary DFT/MD calculations. Movie showing structural changes of the RS-Au-SR staple at RT.

Acknowledgements

This work was supported by the National Natural Science Foundation of China (Grant no. 11604196 and 11574189), Fundamental Research Funds for the Central Universities (Grant no. GK201801005) and Natural Science Foundation of Shaanxi Province (No. 2017JQ1038). J. Gao thanks for the support of National Demonstration

Center for Experimental X-physics Education (Shaanxi Normal University). We also thanks Miss Tiantian Zhao and Miss He Bai for the data collection.

Author contribution:

[§]These authors made equal contributions to the manuscript.

References

[1] Love, J. C.; Estroff, L. A.; Kriebel, J. K.; Nuzzo, R. G.; Whitesides, G. M., Self-assembled monolayers of thiolates on metals as a form of nanotechnology, *Chem. Rev*. **2005**, *105*, 1103.

[2] Kind, M.; Wöll, Ch., Organic surfaces exposed by self-assembled organothiol monolayers: Preparation, characterization, and application, *Prog. Surf. Sci*. **2009**, *84*, 230.

[3] Maksymovych, P.; Voznyy, O.; Dougherty, D. B.; Sorescu, D. V.; Yates, J. T., Jr. , Gold adatom as a key structural component in self-assembled monolayers of organosulfur molecules on Au (111), *Prog. Surf. Sci*. **2010**, *85*, 206.

[4] Schreiber, F., Structure and growth of self-assembling monolayers, *Prog. Surf. Sci*. **2000**, *65*, 151.

[5] Vericat, C.; Vela, M. E.; Benitez, G.; Carro, P.; Salvarezza, R. C., Self-assembled monolayers of thiols and dithiols on gold: new challenges for a well-known system, *Chem. Soc. Rev*. **2010**, *39*, 1805.

[6] Guo, Q.; Li, F., Self-assembled alkanethiol monolayers on gold surfaces: resolving the complex structure at the interface by STM, *Phys. Chem. Chem. Phys*. **2014**, *16*, 19074.

[7] Jadzinsky, P. D.; Careo, G.; Ackerson, C. J.; Bushnell, D. A.; Kornberg, R. D., Structure of a thiol monolayer-protected gold nanoparticle at 1.1 angstrom resolution, *Science*, **2007**, *130*, 3754.

[8] Krishnadas, K. R.; Ghosh, A.; Baksi, A.; Chakraborty, I.; Natarajan, G.; Pradeep,

T., Intercluster Reactions between $Au_{25}(SR)_{18}$ and $Ag_{44}(SR)_{30}$, *J. Am. Chem. Soc.* **2016**, *138*, 140.

[9] Poirier. G. E., Coverage-dependent phases and phase stability of decanethiol on Au (111), *Langmuir* **1999**, *15*, 1167.

[10] Vargas, M. C.; Giannozzi, P.; Selloni, A.; Scoles, G., Coverage-Dependent Adsorption of CH_3S and $(CH_3S)_2$ on Au(111): a Density Functional Theory Study, *J. Phys. Chem. B* **2001**, *105*, 9509.

[11] Ulman, A., Formation and structure of self-assembled monolayers, *Chem. Rev.* **1996**, *96*, 1533.

[12] Poirier, G. E., Characterization of organosulfur molecular monolayers on Au (111) using scanning tunneling microscopy, *Chem. Rev*. **1997**, *97*, 1117.

[13] Kondoh, H.; Iwasaki, M.; Shimada, T.; Amemiya, K.; Yokoyama, T.; Ohta, T.; Shimomura, M.; Kono, S., Adsorption of thiolates to singly coordinated sites on Au (111) evidenced by photoelectron diffraction, *Phys. Rev. Lett*. **2003**, *90*, 066102.

[14] Toerker, M.; Staub, R.; Fritz, T.; Schmitz-Hubsch, T.; Sellam, F.; Leo, K., Annealed decanethiol monolayers on Au (111)–intermediate phases between structures with high and low molecular surface density, *Surf. Sci*. **2000**, *445*, 100.

[15] Nuzzo, R. G.; Dubois, L. H.; Allara, D. L., Fundamental Studies of Microscopic Wetting on Organic Surfaces. 1. Formation and Structural Characterization of a Self-Consistent Series of Polyfunctional Organic Monolayers, *J. Am. Chem. Soc.* **1990**, *112*, 558.

[16] Chidsey, C. E. D.; Liu, G.-Y.; Rowntree, P.; Scoles, G., Molecular order at the surface of an organic monolayer studied by low energy helium diffraction, *J. Chem. Phys.* **1989**, *91*, 4421.

[17] Dishner, M. H.; Hemminger, J. C.; Feher, F. J., Direct observation of substrate influence on chemisorption of methanethiol adsorbed from the gas phase onto the reconstructed Au (111) surface, *Langmuir* **1997**, *13*, 2318.

[18] Kondoh, H.; Kondama, C.; Sumida, H.; Nozoye, H., Molecular processes of adsorption and desorption of alkanethiol monolayers on Au(111), *J. Chem. Phys.* **1999**, 111, 1175.

[19] Dubois, L. H.; Zegarski, B. R.; Nuzzo, R. J. , Molecular ordering of organosulfur compounds on Au (111) and Au (100): Adsorption from solution and in ultrahigh vacuum, *J. Chem. Phys.* **1993**, 98, 678.

[20] Camillone, N.; Leung, T. Y. B.; Schwartz, P.; Eisenberger, P.; Scoles, G., Chain length dependence of the striped phases of alkanethiol monolayers self-assembled on Au (111): An atomic beam diffraction study, *Langmuir* **1996**, *12*, 2737.
[21] Fenter, P.; Eberhardt, A.; Eisenberger, P., Self-assembly of n-alkyl thiols as disulfides on Au (111), *Science* **1994**, *266*, 1216.
[22] Toerker, T. M.; Staub, R.; Fritz, T.; Schmitz-Hübsch, T.; Sellam, F.; Leo, K., Annealed decanethiol monolayers on Au(111) – intermediate phases between structures with high and low molecular surface density, *Surf. Sci.* **2000**, *445* (1), 100.
[23] Maksymovych, P.; Sorescu, D. C.; Yates, J. T., Jr., Gold-adatom-mediated bonding in self-assembled short-chain alkanethiolate species on the Au (111) surface, *Phys. Rev. Lett*. **2006**, *97*, 146103.
[24] Maksymovych, P.; Yates, J. T. Jr, Au adatoms in self-assembly of benzenethiol on the Au (111) surface, *J. Am. Chem. Soc.*, **2008**, *130*, 7518–7519.
[25] Li, F.; Zhou, W-C.; Guo, Q., Uncovering the hidden gold atoms in a self-assembled monolayer of alkanethiol molecules on Au (111), *Phys. Rev. B* **2009**, 79, 113412.
[26] Li, F.; Tang, L.; Voznyy, O.; Gao, J.; Guo, Q., The striped phases of ethylthiolate monolayers on the Au (111) surface: a scanning tunneling microscopy study, *J. Chem. Phys.* **2013**, *138*(19), 194707.
[27] Li, F.; Tang, L.; Gao, J.; Zhou, W-C.; Guo, Q., Adsorption and electron-induced dissociation of ethanethiol on Au (111), *Langmuir* **2012**, *28*(30), 11115-20.
[28] Li, F.; Tang, L.; Zhou, W-C.; Guo, Q, Relationship between the c (4× 2) and the (√ 3×√ 3) R30° phases in alkanethiol self-assembled monolayers on Au (111), *Phys. Chem. Chem. Phys.* **2011**, *13*(25), 11958.
[29] Li, F; Tang, L.; Zhou, W-C.; Guo, Q., Adsorption site determination for Au-octanethiolate on Au (111), *Langmuir* **2010**, *26*, 12, 9484.
[30] Li, F.; Tang, L.; Zhou, W-C.; Guo, Q., The structure of methylthiolate and ethylthiolate monolayers on Au(111): Absence of the (√3×√3)R30° phase, *Surf. Sci.* **2012**, *606*, L31.
[31] Gao, J.; Li, F.; Guo, Mixed methyl-and propyl-thiolate monolayers on a Au (111) Surface, Q. *Langmuir* **2013**, *29* (35), 11082.
[32] Tang, L.; Li, F.; Guo, Q., Complete Structural Phases for Self-Assembled Methylthiolate Monolayers on Au (111), *J. Phys. Chem. C* **2013**, *117* (41), 21234.

[33] Mazzarello, R.; Cossaro, A.; Verdini, A.; Rousseau, R.; Casalis, L.; Danisman, M. F.; Floreano, L.; Scandolo, S.; Morgante, A.; Scoles, G., Structure of a CH_3S Monolayer on Au(111) Solved by the Interplay between Molecular Dynamics Calculations and Diffraction Measurements, *Phys. Rev. Lett*. **2007**, *98*, 16102.

[34] Wang, Y.; Chi,Q.; Hush, N. S.; Reimers, J. R.; Zhang, J.; Ulstrup, J., Scanning tunneling microscopic observation of adatom-mediated motifs on gold− thiol self-assembled monolayers at high coverage, *J. Phys. Chem. C* **2009**, *113*, 19601.

[35] Yu, M.; Bovet, N.; Satterley C. J., *et al*., True nature of an archetypal self-assembly system: Mobile Au-thiolate species on Au (111), *Phys. Rev. Lett*. **2006**, *97*, 166102.

[36] Jiang, D. E.; Dai, S., Cis-trans conversion of the CH3S-Au-SCH3 complex on Au(111), *Phys. Chem. Chem. Phys*. **2009**, *11*, 8601.

[37] Hauptmann, N. Robles, R.; Abufager, P.; Lorente, N.; Berndt, R., AFM Imaging of Mercaptobenzoic Acid on Au(110): Submolecular Contrast with Metal Tips, *J. Phys. Chem. Lett.* **2016**, *7*, 1984.

[38]Hakkinen, H., The gold-sulfur interface at the nanoscale, *Nat. Chem.* **2012**, *4*, 443.

[39] Lofgren, J.; Gronbeck, H.; Moth-Poulsen, K.; Erhrat, P., Understanding the Phase Diagram of Self-Assembled Monolayers of Alkanethiolates on Gold, *J. Phys. Chem. C*. **2016**, *120*, 12059.

[40] Remers, J. R.; Ford, M. J.; Halder, A.; Ulstrup, J.; Hush, N. S., Gold surfaces and nanoparticles are protected by Au(0)–thiyl species and are destroyed when Au(I)–thiolates form, *PNAS*, **2016**, Feb. E1424.

[41] Yan, J.; Ouyang, R.; Jensen, P. S.; Ascic, E.; Tanner, D.; Mao, B.; Zhang, J.; Tang, C.; Hush, N. S.; Ulstryp, J.; Reimers, J. R., Controlling the Stereochemistry and Regularity of Butanethiol Self-Assembled Monolayers on Au(111), *J. Am. Chem. Soc*. **2014**, *136*, 17087.

[42] Clair, S.; Kim, Y.; Kawai, M., Coverage-Dependent Formation of Chiral Ethylthiolate-Au Complexes on Au(111), *Langmuir* **2010**, *27*, 627.

[43] Gao, J., Li, F.; Guo, Q., Balance of Forces in Self-Assembled Monolayers, *J. Phys. Chem. C* **2013**, *117*, 24985

[44] Maksymovych, P.; Yates, J. T., Jr., Au adatoms in self-assembly of benzenethiol on the Au(111) surface, *J. Am. Chem. Soc*. **2008**, *130*, 7518.

[45] Rastgoo-Lahrood, A.; *et al*, From Au–Thiolate Chains to Thioether Sierpiński Triangles: The Versatile Surface Chemistry of 1,3,5-Tris(4-mercaptophenyl)benzene on Au(111), *ACS Nano* **2016**, *10*, 10901.

[46] Heister, K.; Allara, D.; Bahnck, K.; Frey, S.; Zharnikov, M.; Gruze, M., Deviations from 1:1 Compositions in Self-Assembled Monolayers Formed from Adsorption of Asymmetric Dialkyl Disulfides on Gold, *Langmuir* **1999**, *15*, 5440.

[47] Heinecke, C. L.; Ni, T. W.; Malola, S.; Makinen, V.; Wong, O. A.; Hakkinen, H.; Ackerson, C. J., Structural and Theoretical Basis for Ligand Exchange on Thiolate Monolayer Protected Gold Nanoclusters, *J. Am. Chem. Soc*. **2012**, *134*, 13316.

[48] Maksymovych, P.; Sorescu, D. C.; Voznyy, O.; Yates, J. T., Jr., Hybridization of phenylthiolate- and methylthiolate-adatom species at low coverage on the Au(111) surface, *J. Am. Chem. Soc.* **2013**, *135*, 4922.

[49] Kresse, G.; Hafner, J., *Ab initio* molecular dynamics for open-shell transition metals, *Phys. Rev. B* **1993**, *48*, 13115.

[50] Kresse, G.; Hafner, J., *Ab initio* molecular-dynamics simulation of the liquid-metal-amorphous-semiconductor transition in germanium, *Phys. Rev. B* **1994**, *49*, 14251.

[51] Kresse, G.; Joubert, D., From ultrasoft pseudopotentials to the projector augmented-wave method, *Phys. Rev. B* **1999**, *59*, 1758.

[52] Elmér, R.; Berg, M.; Carlén, L.; Jakobsson, B.; Norén, B.; Oskarsson, A.; Ericsson, G.; Julien, J.; Thorsteinsen, T. F.; Guttormsen, M.; Løvhøiden, G.; Bellini, V.; Grosse, E.; Müntz, C.; Senger, P.; Westerberg, L., K+ Emission in Symmetric Heavy Ion Reactions at Subthreshold Energies, *Phys. Rev. Lett*. **1997**, *78*, 1396.

[53] Dion, M.; Rydberg, H.; Schröder, E.; Langreth, D. C.; Lundqvist, B. I., Van der Waals density functional for general geometries, *Phys. Rev. Lett*. **2004**, *92*, 246401.

[54] Román-Pérez, G.; Soler, J. M., Energetics and Dynamics of H_2 Adsorbed in a Nanoporous Material at Low Temperature, *Phys. Rev. Lett*. **2009**, *103*, 096102.

[55] Klimeš, J.; Bowler, D. R., Van der Waals density functionals applied to solids, *Phys. Rev. B* **2011**, *83*, 195131.

[56] Tersoff, J., Role of tip electronic structure in scanning tunneling microscope images, *Phys. Rev. B* **1990**, *41*, 1235.

[57] Hofer, W. A.; Foster, A. S.; Shluger, A. L., Theories of scanning probe microscopes at the atomic scale, *Rev. Modern Phys.* **2003**, *75*, 1287.

[58] Gao, J.; Li, F.; Zhu, G-Q.; Lin, H-P.; Li, Q; Li, Y-Y.; Pan, M; Guo, Q. **2018**,

Supplementary Information.

[59] Gao, J.; Tang, L.; Holmes, S.; Li, F.; Palmer, R. E.; Guo, Q., Surface-induced symmetry reduction in molecular switching: asymmetric *cis–trans* switching of CH_3S-Au-SCH_3 on Au(111), *Nanoscale* **2016**, *8*, 19787.

TOC Graphic

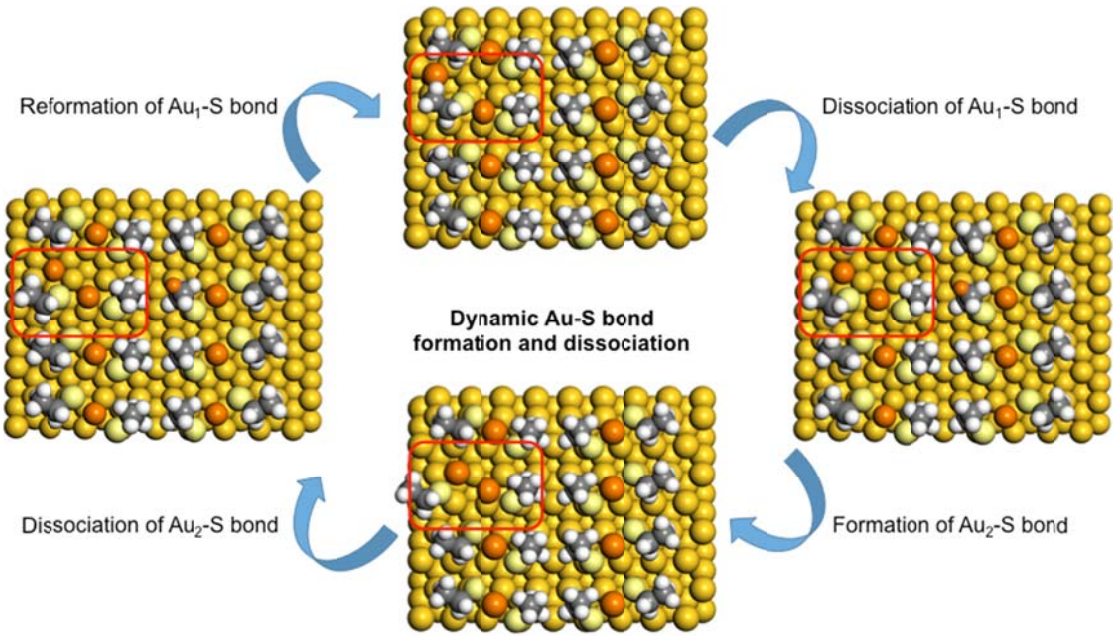
Reformation of Au_1-S bond
Dissociation of Au_1-S bond
Dynamic Au-S bond
formation and dissociation
Dissociation of Au_2-S bond
Formation of Au_2-S bond